

Summary of an Active Flexible Wing Program

Boyd Perry III* and Stanley R. Cole†
NASA Langley Research Center, Hampton, Virginia 23681
and

Gerald D. Miller‡
Rockwell International Corporation, Los Angeles, California 90009

This article presents a summary of a NASA/Rockwell Active Flexible Wing program. Major elements of the program are presented. Key program accomplishments included single- and multiple-mode flutter suppression, load alleviation and load control during rapid roll maneuvers, and multi-input/multi-output multiple-function active controls tests above the open-loop flutter boundary.

Introduction

IN the mid1980s Rockwell International Corporation pioneered and advanced a concept named the Active Flexible Wing (AFW) concept.¹ This concept exploited, rather than avoided, wing flexibility to provide weight savings and improved aerodynamics for advanced fighter configurations. In the AFW concept, weight savings were realized in two ways: 1) a flexible wing and 2) no horizontal tail.

In an AFW wing design large amounts of aeroelastic twist are permitted in order to provide improved maneuver aerodynamics at several design points (subsonic, transonic, and supersonic). However, a direct result of these large amounts of twist is degraded roll performance (in the form of aileron reversal) over a significant portion of the flight envelope. At this point in a typical fighter design, a "rolling tail" would be added to the vehicle to provide acceptable roll performance. However, in an AFW design, multiple leading- and trailing-edge wing control surfaces are used in various combinations, up to and beyond reversal, to provide acceptable roll performance. For such a design an active roll control (ARC) system^{1,2} is required to efficiently manage the rolling of the vehicle. An ARC system monitors flight conditions and, based on those conditions, chooses the most effective control surfaces to roll the vehicle, and also chooses the proper sign for control-surface deflections (one sign if below reversal, the opposite if above).

In an AFW design, further weight savings could also be achieved by the additional use of active controls. Taken alone or in combination, flutter suppression, gust load alleviation, and maneuver load alleviation all have the potential for further reductions in vehicle weight. By taking full advantage of active controls and the AFW concept, Rockwell predicted that weight savings of at least 15% of takeoff gross weight could be achieved for an advanced fighter configuration.¹

The Active Flexible Wing program grew out of the AFW concept. The test-bed for the AFW program was the aero-

elastically-scaled wind-tunnel model of an advanced fighter configuration shown in Fig. 1. The model, referred to as the AFW wind-tunnel model, was designed and built by Rockwell and tested on four different occasions in the NASA Langley Transonic Dynamics Tunnel (TDT). Since 1985 there have actually been two independent AFW programs. Both programs have been called "the AFW program" and both have had two wind-tunnel tests using the AFW wind-tunnel model. To date, no deliberate attempt has been made to clearly distinguish between the two programs. This and the next two paragraphs represent such an attempt.

The first AFW program involved the U.S. Air Force, NASA, and Rockwell International. The goal of this program was to demonstrate the AFW concept. Two wind-tunnel tests (one in 1986 and one in 1987) were conducted in support of this goal, and the results from these tests are reported in Refs. 1 and 2.

The second AFW program involved only NASA and Rockwell International. The goal of this program was the demonstration of aeroelastic control (consistent with the AFW concept) through the application of digital active controls technology. Two wind-tunnel tests (1989 and 1991), were conducted in support of this goal. The remainder of this article and Refs. 3–12 deal only with the second AFW program, with major emphasis on the 1991 wind-tunnel test.

Test Apparatus

Wind Tunnel

The AFW wind-tunnel tests were conducted in the NASA Langley TDT.¹³ The TDT is a closed-circuit, continuous-flow wind tunnel capable of testing at stagnation pressures from near zero to atmospheric, and over a Mach number range from 0 to 1.2. The test section of the TDT is 16 ft² with cropped corners. The TDT is capable of testing with either an air or a heavy gas test medium. The 1986 and 1987 wind-tunnel entries of the AFW model utilized the heavy gas test medium.

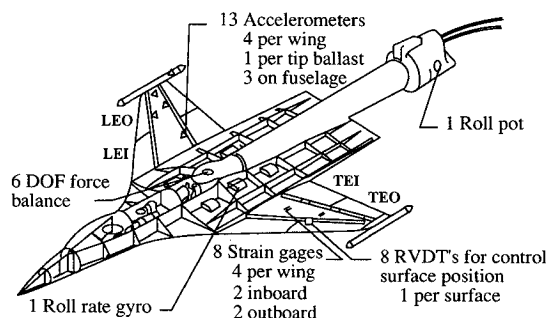


Fig. 1 Schematic of AFW wind-tunnel model.

Presented as Paper 92-2080 at the Dynamic Specialist Conference, Dallas, TX, April 16–17, 1992; received May 10, 1992; revision received March 7, 1994; accepted for publication March 21, 1994. Copyright © 1994 by the American Institute of Aeronautics and Astronautics, Inc. No copyright is asserted in the United States under Title 17, U.S. Code. The U.S. Government has a royalty-free license to exercise all rights under the copyright claimed herein for Governmental purposes. All other rights are reserved by the copyright owner.

*Assistant Head, Aeroelasticity Branch, Structures Division, M/S 340.

†Aeroelasticity Branch, Structures Division, M/S 340. Senior Member AIAA.

‡Program Manager, North American Aircraft, P.O. Box 92098, M/S GB01.

The 1989 and 1991 entries were conducted with an air test medium.

A feature of the TDT that is particularly useful for aeroelastic testing is a group of four bypass valves connecting the test section area (plenum) of the tunnel to the opposite leg of the wind-tunnel circuit downstream of the drive fan motor. In the event of a model instability, such as flutter, these quick-actuating valves are opened, causing a rapid reduction in the test section Mach number and dynamic pressure, which may result in stabilizing the model. During the AFW wind-tunnel tests, instrumentation on the model was monitored using electronic equipment that could automatically command the bypass valves to open if model response exceeded a predetermined criteria of amplitude and frequency.

Wind-Tunnel Model

The AFW wind-tunnel model was a full-span, aeroelastically-scaled representation of a fighter aircraft configuration. It had a low-aspect ratio wing with a span of 8.67 ft. The model was supported on the wind-tunnel test section centerline by a sting mount specifically constructed for the AFW wind-tunnel model. This sting utilized an internal ball-bearing arrangement to allow the model freedom to roll about the sting axis. The fuselage was connected to the sting through a pivot arrangement so that the model could be remotely pitched from approximately -1.5 - to $+13.5$ -deg angle of attack. A schematic of the wind-tunnel model is shown in Fig. 1.

Control Surfaces

The model had two leading-edge and two trailing-edge control surfaces on each wing panel. Each control surface had a chord and span of 25% of the local chord, and 28% of the wing semispan, respectively. The control surfaces were connected to the wing by hinge-line-mounted, vane-type rotary actuators powered by an onboard hydraulic system. Deflection limits of ± 10 deg were imposed on the control surfaces to avoid exceeding hinge-moment and wing-load limitations.

Tip Ballast Store

The original AFW model was modified before the 1989 wind-tunnel test to move its flutter boundary into the operating envelope of the TDT. This modification consisted of adding a ballast store to each wingtip. A drawing of the tip store is shown in Fig. 2. The ballast was basically a thin, hollow aluminum tube with internal ballast distributed to lower the basic wing flutter boundary to a desired dynamic pressure range. Additionally, the store provided a model safety feature. Instead of a hard attachment, the store was connected to the wing by a pitch-pivot mechanism. The pivot allowed freedom for the tip store to pitch relative to the wing surface. When testing for flutter, an internal hydraulic brake held the store to prevent such rotation. This was called the "coupled" tip ballast store configuration. In the event of a flutter instability, this brake was released. In the released, or "decoupled," configuration the pitch stiffness of the store was provided by a spring element internal to the store as shown in Fig. 2. The reduced stiffness of the spring element, as compared to the hydraulic brake arrangement, significantly increased the frequency of the first torsion mode of the wing. This change in frequency moved the flutter condition to higher

dynamic pressures. This behavior was related to the concept of the decoupler pylon as discussed in Ref. 14.

Instrumentation

The AFW model was instrumented with a six-component, force-and-moment balance, accelerometers, strain-gauge bridges, rotary variable differential transducers (to measure control surface deflection angles), a roll potentiometer, and a roll-rate gyro.

Digital Controller

An important objective of the AFW program was to gain practical experience in designing, fabricating, and implementing a real-time multi-input/multi-output (MIMO) multiple-function digital controller, and in developing the hardware interface between the controller and the wind-tunnel model. Required features of the digital controller were that 1) it be representative of a digital controller on a full-scale airplane, 2) control laws could be easily modified and/or replaced, 3) it be capable of simultaneous execution of flutter suppression control laws and rolling maneuver control laws and 4) it be capable of receiving and sending both analog and discrete signals. Additional capabilities of the digital controller included the manual positioning of the control surfaces, the calculation and application of excitation signals to various control surfaces, and the recording, transferring, and storing of digitized signals.

To meet these requirements with reasonable resources, a SUN 3/160 workstation driven by a Unix operating system was selected as the "shell" of the digital controller. The hardware components of the digital controller included a host computer, two digital signal processor (DSP) boards, an array processor (AP) board, two analog-to-digital, and two digital-to-analog conversion boards. A "primary system" and a "backup system" were configured from these components, affording some degree of redundancy in case of a failure of one of the processor boards.

Most software was written in the high level C programming language. A generic form of the control-law structure was identified such that one set of software would accommodate a given control law while imposing minimal constraints on the control-law designers. The generic form of the control-law function allowed for changes in a design to be implemented easily and reliably. Reference 5 presents a detailed description of the AFW digital controller.

Analytical Representations of AFW Wind-Tunnel Model

This section of the article outlines the development at NASA Langley of the aeroelastic equations of motion for the AFW wind-tunnel model. The wind-tunnel model had four possible configurations defined by the four possible combinations of two features (roll freedom and tip ballast store), as indicated in Table 1. Because equations were required for many combinations of Mach number and dynamic pressure, and because there were a variety of anticipated uses for the equations, a significant engineering effort was expended, resulting in an extensive data base of aeroelastic equations of motion. This section of the article outlines the development at NASA Langley of the aeroelastic equations of motion for the AFW wind-tunnel model.

Table 1 Model configurations

	Model configuration number for tip ballast store	
	Coupled	Uncoupled
Fixed in roll	1	2
Free to roll	3	4

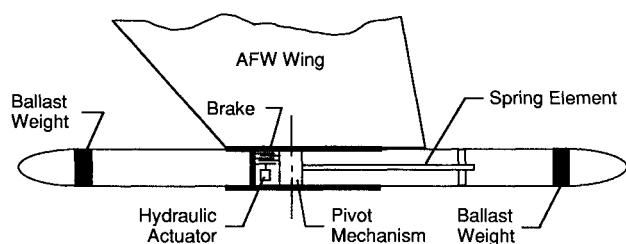


Fig. 2 Drawing showing details of tip ballast store.

Linear Aeroelastic Equations of Motion

The starting point for all equations of motion was a Rockwell-generated finite element model of the AFW wind-tunnel model. An eigensolver analysis was employed to obtain the mode shapes, frequencies, and generalized masses for the first 10 symmetric and the first 10 antisymmetric elastic modes. Control-surface-deflection modes were appended to all configurations, and a rigid-body roll mode was appended to configurations 3 and 4 in Table 1.

Linear aeroelastic equations of motion were created using the ISAC code.¹⁵ Subsonic generalized aerodynamic forces due to motion and gust were computed using a doublet-lattice technique¹⁶ within ISAC, and then combined with generalized stiffness, damping, and mass matrices to form second-order, reduced-frequency-dependent aeroelastic equations of motion. Flutter calculations were performed by using these equations with the solution techniques described in Ref. 17. Rational function approximations to the generalized aerodynamic forces permitted a recasting of these equations into first-order linear-time-invariant state-space equations. These first-order equations were then made available for control-law design.

The following corrections and refinements were made in an effort to improve the quality of the linear aeroelastic equations of motion:

- 1) Modal frequencies measured during ground vibration tests were substituted for corresponding analytically computed frequencies.
- 2) Parameter estimation techniques were employed to create analytical representations of measured electrohydraulic control-surface actuator transfer functions. For each actuator pair, an averaged right-side-plus-left-side transfer function was incorporated into the equations.
- 3) Correction factors for control-surface effectiveness terms (functions of dynamic pressure, derived by comparing wind-tunnel data with corresponding analytical quantities) were applied to all control-surface generalized aerodynamic forces.

Nonlinear Simulation of Aeroelastic Equations of Motion

Two nonlinear simulations were employed to support preparations for the 1989 and 1991 wind-tunnel entries: 1) a comprehensive nonlinear batch simulation and 2) a nonlinear hot-bench simulation. This section of the article briefly describes each.

Batch Simulation

The nonlinear batch simulation served as a "truth model" for control law designers in the evaluation of control laws prior to wind-tunnel tests. The starting point for the batch simulation was the linear equations of motion and their corresponding corrections and refinements. Further refinements were incorporated so that asymmetries and nonlinearities could be included into the truth model. By dropping the assumption of planes of symmetry and antisymmetry, the aeroelastic equations of motion were rewritten as "whole aircraft" equations, thereby allowing the right-side and left-side actuators to be modeled individually. In addition, actuator rate limits as functions of load were incorporated. The batch simulation also modeled the characteristics of electronic equipment. The dynamics of anti-aliasing filters were included, as were quantization effects and computational delays associated with the digital controller. The batch simulation used a Runge-Kutta second-order predictor-corrector formula to integrate all state derivatives. The integration step size was 0.0005 s. Reference 3 contains a detailed description of the nonlinear batch simulation.

Hot Bench Simulation

The purpose of the Hot Bench Simulation (HBS) was to verify the functionality and the operation of the digital controller before actual testing in the wind tunnel. The HBS was used to uncover sign errors, errors in logic, and other software errors, as well as system faults and other hardware errors.

The HBS was implemented in real time using the Langley Advanced Real-Time Simulation (ARTS) system.¹⁸ The ARTS system consists of two Cyber 175 computers connected to an array of simulation sites by means of a 50-Mbit/s fiber optic digital data network. The nonlinear whole aircraft aeroelastic equations of motion, transferred from the batch simulation, resided on the Cybers. Actuator commands from the digital controller were sent over the network and became inputs to the aeroelastic equations on the Cybers. In turn, wind-tunnel model response quantities (which were used as sensor signals for control laws residing in the digital controller), were sent back over the network to the digital controller. The HBS ran at a synchronized real time of 5:1 "slow."

The HBS also provided valuable practice for the human operators of the digital controller. A Terabit Eagle 1000 graphics computer, interfaced directly to the Cyber 175, was used to generate a color-coded, three-dimensional wire-frame outline of the AFW model. Reference 3 contains a detailed description of the HBS.

Nonlinear Aerodynamic Analysis

Transonic flutter testing was performed during the 1989 entry. For analytical guidance during testing, it was deemed desirable to perform flutter calculations prior to testing using the Computational Aeroelasticity Program-Transonic Small Disturbance (CAP-TSD) code.¹⁹ CAP-TSD solves the (nonlinear) transonic small disturbance equation using a time-accurate, approximate factorization algorithm. CAP-TSD can handle realistic configurations with multiple lifting surfaces, control surfaces, vertical surfaces, bodies, and a fuselage. Reference 4 describes the calculation of the symmetric flutter boundary used as guidance during the 1989 entry, further refinements to that analysis, and a more recent antisymmetric flutter analysis.

Control Law Design

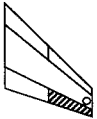
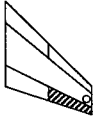
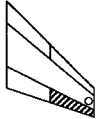
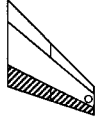
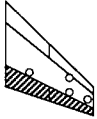
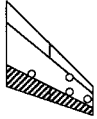
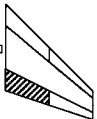
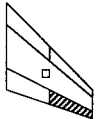
Two kinds of control laws were designed and tested on the AFW wind-tunnel model: 1) flutter suppression control laws and 2) rolling maneuver control laws. Four teams designed flutter suppression control laws; two teams designed rolling maneuver control laws. This section of the article states the design objectives and goals for each kind of control law, and briefly describes the design procedures and control laws produced by all six design teams for the 1991 entry.

Flutter Suppression Control Laws

The design objective of the flutter suppression control laws was to develop low-order robust digital control laws that would simultaneously suppress symmetric and antisymmetric flutter and operate in conjunction with rolling maneuver control laws. The design goal was to increase the lowest open-loop flutter dynamic pressure by 30% (the tunnel limit). Specifications were developed to reflect required levels of robustness. Singular-value based MIMO multiplicative stability margins corresponding to ± 6 -dB gain margin and ± 45 -deg phase margin were required over the entire test dynamic pressure range to account for modeling errors and uncertainties. (These requirements were subsequently relaxed to ± 4 dB and ± 30 deg.) Sensitivity analyses were also required to assure that likely modeling errors and uncertainty effects could be accommodated by the flutter suppression control laws. Acceptable control-surface deflections and rates were also required.

Flutter suppression control laws (also referred to as flutter suppression systems—FSS) were designed for two model configurations: 1) fixed-in-roll and 2) free-to-roll. For the fixed-in-roll configuration, two flutter modes (symmetric and antisymmetric) had to be suppressed in order to demonstrate even a modest increase in flutter dynamic pressure. Therefore, both symmetric and antisymmetric FSS were required. For the free-to-roll configuration only one flutter mode (symmetric) had to be suppressed, and consequently, only a sym-

Table 2 Flutter suppression control law description

Synthesis methods	Symmetric		Antisymmetric	
	Controls/sensors	Control law order	Controls/sensors	Control law order
FSS 1		5th		5th
FSS 2		3rd		3rd
FSS 3		11th		8th
FSS 4		3rd		7th

○ Accelerometer. □ Strain gauge.

metric FSS was required. The symmetric FSS designed by each team was used for both fixed-in-roll and free-to-roll model configurations.

Methods used in the design of flutter suppression control laws (and an acronym for each) are:

- FSS 1 = reduced-order linear quadratic Gaussian design
- FSS 2 = traditional pole/zero design
- FSS 3 = MIMO constrained optimization design
- FSS 4 = classical design with strain gauge feedback

Table 2 contains a summary of the control surfaces, sensors, and the order of all symmetric and antisymmetric flutter suppression control laws. References 7–10 contain the details of the FSS designs and comparisons of analytical predictions and experimental results.

Rolling Maneuver Control Laws

The design objective of these control laws was to reduce or limit wing loads during rolling maneuvers of 90 deg. Important design considerations were to maintain stability, acceptable control surface activity, and constant roll performance. These control laws were implemented with the wind-tunnel model in the free-to-roll configuration.

Rolling Maneuver Load Alleviation

The approach taken in the design of the rolling maneuver load alleviation (RMLA) system was to employ classical techniques using gain feedback and low-pass filters. To quantify the level of load reduction achieved by the RMLA system, a baseline system was also designed and tested. (No attempt to reduce loads was made in the design of the baseline system.) The RMLA system used the roll rate gyro as the sensor and two pairs of control surfaces.

Roll Rate Tracking System

The approach taken in the design of the RRTS was to employ constrained optimization to create a series of look-up tables that served to limit loads only when the loads reached a predetermined level. (Below this level, no attempt was made to limit loads.) These look-up tables contained values of control surface deflection as functions of the measured roll rate

and values of the difference between the measured and the commanded roll rates. The tables resided in the forward path of the control system. The RRTS used the roll rate gyro as the sensor and three pairs of control surfaces.

References 11 and 12 contain the details of the rolling maneuver control law designs and comparisons of analytical predictions and experimental results.

On-Line Analysis Capabilities

A variety of on-line analysis capabilities were developed for and successfully used during the 1989 and 1991 wind-tunnel entries. These capabilities provided valuable quantitative information about the wind-tunnel model and its active control systems. Based on this information, decisions could be made to continue with a particular test, to alter a test, or even to terminate a test, thereby contributing to the overall safety of the wind-tunnel model. The on-line analysis capabilities also provided an early qualitative indication of the success of the current tests. Major capabilities included the following: control law validation, controller performance evaluation, plant estimation, time-history plots, and rms calculations. Reference 6 describes the on-line analysis capabilities in detail and presents examples of each.

Test Results

This section of the article presents a summary of test results from the 1989 and 1991 wind-tunnel entries. These results are categorized as open-loop flutter tests (flutter boundary determination), single-function active controls tests (flutter suppression only and rolling maneuver only), and multiple-function active controls tests (flutter suppression and rolling maneuver simultaneously). Single-function testing was performed before multiple-function testing.

Open-Loop Flutter Testing

Open-loop flutter conditions were needed to assess the performance of the flutter suppression control laws, as well as to assess model safety risks throughout the wind-tunnel tests. A plot of the measured open-loop flutter conditions, determined by several subcritical response techniques, is shown in Fig. 3. The transonic symmetric flutter conditions shown were obtained during the 1989 entry. The subsonic antisymmetric and symmetric flutter conditions shown in the figure were measured during the 1991 entry. During the 1991 entry, all testing was at atmospheric pressure conditions due to operating limitations of the facility at the time of the test entry. Figure 3 also shows the maximum subsonic condition to which the decoupled tip ballast store configuration was tested, and corresponds to the maximum dynamic pressure that could be attained in the TDT with the AFW model installed. (The tunnel operating boundary shown in Fig. 3 is for an empty test section.) The decoupled configuration was tested to conditions 32% (in terms of dynamic pressure) beyond the antisymmetric-flutter condition, and 23% beyond the symmetric-flutter condition of the coupled configuration. This indicates the effectiveness of the tip ballast stores in providing a

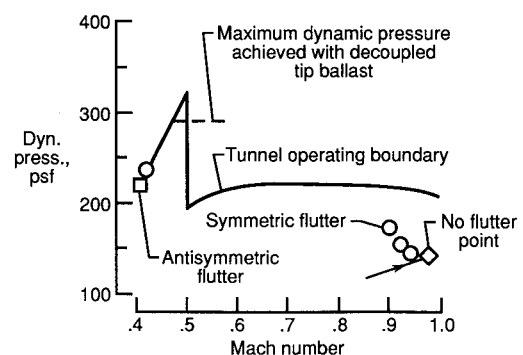


Fig. 3 Open-loop flutter conditions.

passive backup safety system in the event of an unanticipated violent flutter condition.

Single-Function Active Controls Testing—Flutter Suppression

Flutter-suppression tests on the AFW wind-tunnel model were conducted on the free-to-roll configuration and on the fixed-in-roll configuration. Figure 4 contains a summary of the flutter-suppression testing that was accomplished during the 1991 entry.

Free-to-Roll Configuration

To suppress flutter in this model configuration, a control law had to suppress only one flutter mode: symmetric. Each of the four flutter-suppression control laws were tested successfully in this model configuration. Figure 4a shows that all four control laws were able to suppress flutter to a dynamic pressure condition 23% beyond the symmetric flutter dynamic pressure. However, this percentage increase did not represent encountering the closed-loop flutter boundary. Testing was ceased at this dynamic pressure condition due to the operating limits of the facility. All four control laws were stabilizing the model at this condition.

Fixed-in-Roll Configuration

To suppress flutter in this model configuration, a control law had to suppress two flutter modes: 1) symmetric and 2) antisymmetric. Therefore, both symmetric and antisymmetric flutter-suppression control laws had to be operating simultaneously. Only three of the flutter-suppression control laws were tested in this model configuration; the fourth was unable to be tested. Figure 4b presents the results. In each of these cases, the control laws were able to function while simultaneously suppressing both the symmetric and the antisymmetric flutter modes at conditions up to 26% beyond the antisymmetric-open-loop flutter dynamic pressures, and up to 17% beyond the symmetric-open-loop flutter dynamic pressures. Maximum test conditions were limited by high dynamic response of the wing surfaces for all of the flutter-suppression control laws tested. However, analysis of the experimental measurements indicates that each control law was still stabilizing both flutter modes at these maximum conditions.

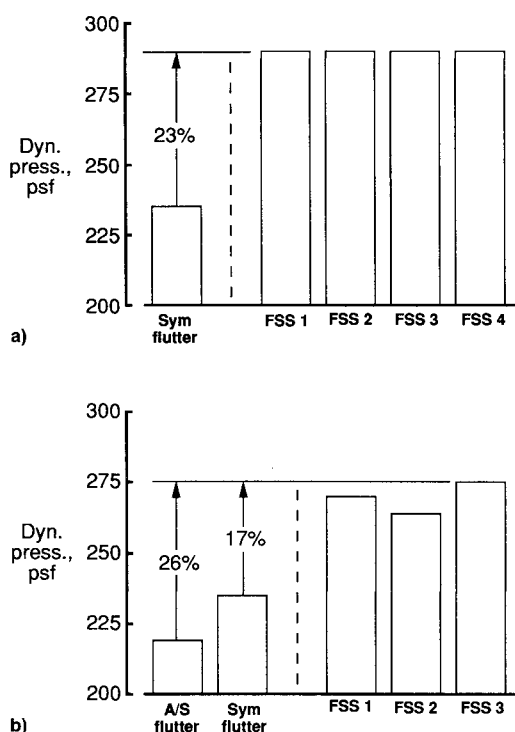


Fig. 4 Flutter-suppression results: a) free-to-roll and b) fixed-in-roll flutter suppressions.

Single-Function Active Controls Testing—Rolling Maneuver

Two RMLA control laws and an RRTS control law were tested separately during the 1991 entry. In the coupled configuration, RMLA and RRTS control laws were tested below the open-loop symmetric flutter condition. In the decoupled configuration, RMLA control laws were tested at a dynamic pressure of 250 psf, and the RRTS control law was tested at 250 and 290 psf.

Figure 5 shows a typical result from RMLA single-function testing. An RMLA control law and a baseline control law were each employed separately, and, as indicated by the roll time histories in Fig. 5a, each resulted in nearly identical roll maneuvers. (The dashed vertical line indicates the end of the maneuver.) However, as shown in Fig. 5b, the resulting time histories of incremental outboard torsion moment were significantly different. The peak value of this load was reduced by more than 50% by the RMLA control law. A more complete presentation of results from RMLA testing may be found in Ref. 11.

Figure 6 shows results representative of RRTS single-function testing. It contains comparisons of analytical predictions and test results during a roll maneuver at a dynamic pressure of 250 psf. The RRTS system had the feature that wing loads were controlled only when they exceeded some specified level. The roll-rate time histories in Fig. 6a indicate a roll maneuver with aggressive accelerations and decelerations. The tor-

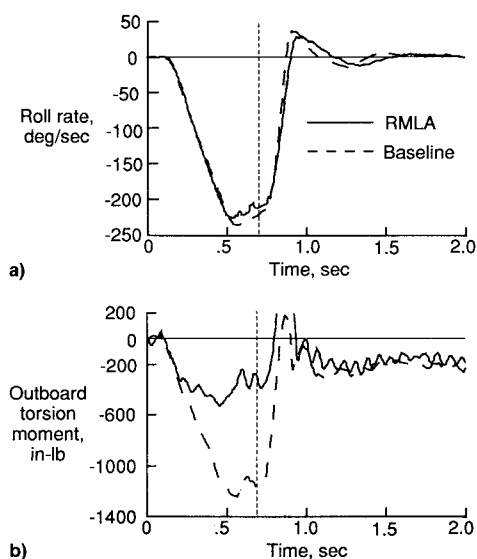


Fig. 5 Typical RMLA performance: a) roll rate and b) torsional moment comparisons.

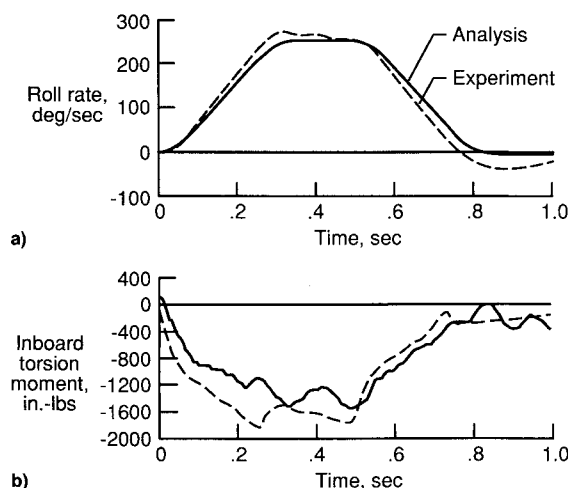


Fig. 6 Typical RRTS performance: a) roll rate and b) torsion moment comparisons.

Table 3 Maximum test conditions for multifunction control law testing

Control laws	Maximum test conditions q , psf	
	Cruise	Rolling maneuver
RRTS + FSS 2	290	275
RRTS + FSS 3	290	260
RRTS + FSS 4	290	260
RMLA + FSS 1	290	260

sion moment time histories in Fig. 6b show that torsion moments were kept within about ± 1400 in.-lb analytically, and within about ± 1800 in.-lb experimentally. A more complete presentation of results from RRTS testing may be found in Ref. 12.

Multiple-Function Active Controls Testing

An important goal of the AFW program was the demonstration of MIMO multiple-function control law testing. Multiple-function control was accomplished through the simultaneous operation of flutter suppression and rolling maneuver control laws. Four combinations of flutter suppression and rolling maneuver control laws were tested. The wind-tunnel model was in the free-to-roll configuration, and for this reason only the symmetric flutter mode had to be suppressed. Two types of multiple-function tests were performed: "cruise" and "rolling maneuver." A summary of the different control law combinations that were tested and the corresponding maximum dynamic pressure test conditions achieved is presented in Table 3.

Cruise

In this type of testing flutter suppression and rolling maneuver control laws were operated simultaneously, but no roll maneuvers were performed. As can be seen from the second column in Table 3, all four combinations of flutter suppression and rolling maneuver control laws remained fully operational up to the maximum dynamic pressure conditions attainable in the TDT, demonstrating a 23% increase in flutter dynamic pressure.

Rolling Maneuver

In this type of testing, flutter suppression and rolling maneuver control laws were operated simultaneously, and rapid roll maneuvers were performed. These same combinations of control laws demonstrated rolling maneuvers above the open-loop symmetric flutter boundary. Most of these demonstrations were conducted at or below a dynamic pressure of 260 psf, with one rolling maneuver being demonstrated at a dynamic pressure of 275 psf for one combination of control laws. Based on these conditions, rolling maneuvers were performed at dynamic pressures 11–17% above the symmetric flutter boundary for four different combinations of flutter suppression and rolling maneuver control laws.

Concluding Remarks

This article has presented a summary of a NASA/Rockwell AFW program, with emphasis on the 1991 wind-tunnel test. Major elements of the program, hardware, software, control law design methods, and test results, have been presented. Key program accomplishments included single- and multiple-mode flutter suppression, load alleviation and load control during rapid roll maneuvers, and multi-input/multi-output

multiple-function active control tests above the open-loop flutter boundary. Other accomplishments that were essential to the overall success of the program were the design, fabrication, and successful operation of the tip ballast store; the design, fabrication, coding, and successful operation of the digital controller in which the flutter suppression and rolling maneuver control laws were executed; the design and execution of two simulation methods: 1) to check the functionality of the digital controller, and 2) to aid the control law designers in their task; and the development and successful operation of a methodology for on-line controller performance evaluation.

References

- Miller, G. D., "Active Flexible Wing (AFW) Technology," Air Force Wright Aeronautical Labs., AFWAL-TR-87-3096, Feb. 1988.
- Perry, B., III, Dunn, H. J., and Sandford, M. C., "Control Law Parameterization for an Aeroelastic Wind-Tunnel Model Equipped with an Active Roll Control System and Comparison with Experiment," AIAA Paper 88-2211, April 1989.
- Buttrill, C. S., Bacon, B. J., Heeg, J., Houck, J. A., and Wood, D., "Simulation and Model Reduction for the AFW Program," AIAA Paper 92-2081, April 1992.
- Silva, W. A., and Bennett, R. M., "Further Investigations of the Aeroelastic Behavior of the AFW Wind-Tunnel Model Using Transonic Small Disturbance Theory," AIAA Paper 92-2082, April 1992.
- Hoadley, S. T., and McGraw, S. M., "The Multiple-Function Multi-Input/Multi-Output Digital Controller System for the AFW Wind-Tunnel Model," AIAA Paper 92-2083, April 1992.
- Wieseman, C. D., Hoadley, S. T., and McGraw, S. M., "On-Line Analysis Capabilities Developed to Support the AFW Wind-Tunnel Tests," AIAA Paper 92-2084, April 1992.
- Mukhopadhyay, V., "Flutter Suppression Digital Control Law Design and Testing for the AFW Wind-Tunnel Model," AIAA Paper 92-2095, April 1992.
- Christhilf, D. M., and Adams, W. M., Jr., "Multifunction Tests of a Frequency Domain Based Flutter Suppression System," AIAA Paper 92-2096, April 1992.
- Waszak, M. R., "Flutter Suppression for the Active Flexible Wing: Control System Design and Experimental Validation," AIAA Paper 92-2097, April 1992.
- Klepl, M. J., "A Flutter Suppression System Using Strain Gauges Applied to Active Flexible Wing Technology: Design and Test," AIAA Paper 92-2098, April 1992.
- Woods-Vedeler, J. A., and Pototzky, A. S., "Rolling Maneuver Loads Alleviation Using Active Controls," AIAA Paper 92-2099, April 1992.
- Moore, D. B., "Maneuver Load Control Using Optimized Feed-forward Commands," AIAA Paper 92-2100, April 1992.
- Reed, W. H., III, "Aeroelasticity Matters: Some Reflections of Two Decades of Testing in the NASA Langley Transonic Dynamics Tunnel," NASA TM-83210, Sept. 1981.
- Reed, W. H., III, Foughner, J. T., Jr., and Runyan, H. L., Jr., "Decoupler Pylon: A Simple, Effective Wing/Store Flutter Suppressor," *Journal of Aircraft*, Vol. 17, No. 3, 1980, pp. 206–211.
- Adams, W. M., Jr., and Hoadley, S. T., "ISAC: A Tool For Aeroservoelastic Modeling and Analysis," NASA TM-109031, Dec. 1993.
- Giesing, J. P., Kalman, T. P., and Rodden, W. P., "Subsonic Unsteady Aerodynamics for General Configurations, Part I. Direct Application of the Nonplanar Doublet Lattice Method," Air Force Flight Dynamics Lab., AFFDL-TR-71-5, Vol. I, Nov. 1971.
- Adams, W. M., Jr., Tiffany, S. H., Newsom, J. R., and Peele, E. L., "STABCAR—A Program for Finding Characteristic Roots of Systems Having Transcendental Stability Matrices," NASA TP 2165, June 1984.
- Crawford, D. J., Cleveland, J. I., II, and Staib, R. O., "The Langley Advanced Real-Time Simulation (ARTS) System Status Report," AIAA Paper 88-4595, Sept. 1988.
- Batina, J. T., "Efficient Algorithm for Solution of the Unsteady Transonic Small-Disturbance Equation," *Journal of Aircraft*, Vol. 25, No. 7, 1988, pp. 598–605.